EWASS-2019

Обзор отдельных результатов
от Сильченко ОК

Глубокие обзоры: LEGA-C (van der Wel)

- VLT+HST, глубокие спектры + imaging
- > 3000 галактик в интервале 0.6<z<1.0 (второй релиз был в августе 2018 года)
- Диапазон масс 10.0<log M_*<11.5
- S/N>20, спектральное разрешение 4500
- Индикаторы свойств звездного населения – H-delta и D_{4000}
- По возрасту населения бимодальность отлично видна уже на z=1

Выборка

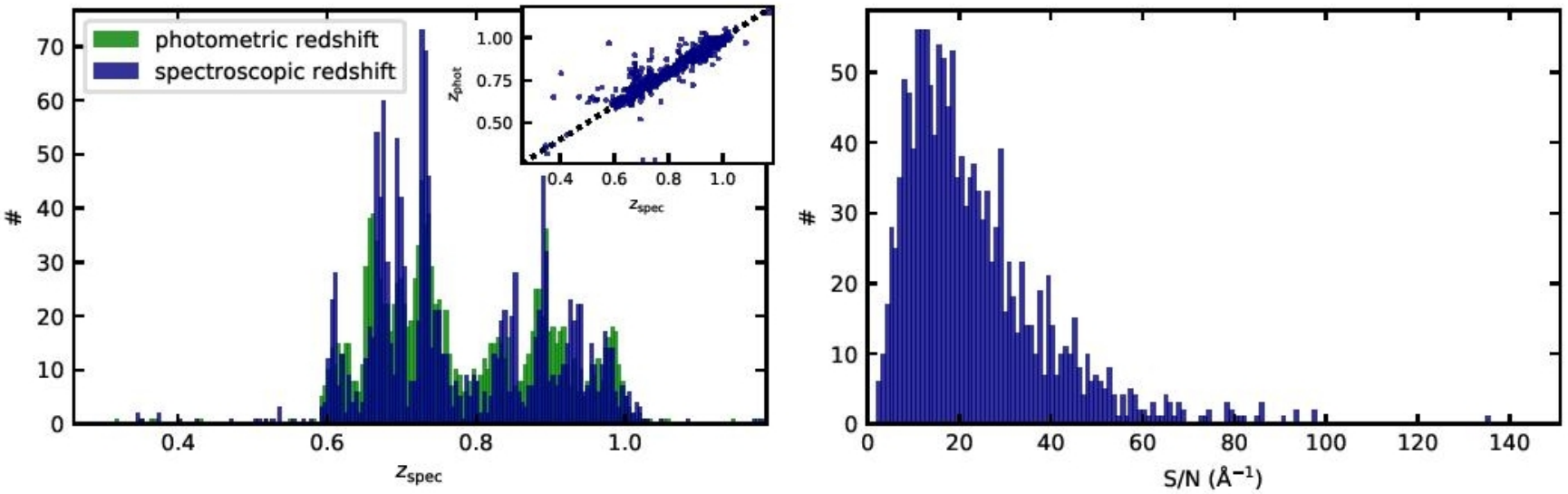

Figure 3. Left: the distribution of spectroscopic redshifts (darkblue histogram) within DR2 of primary targets with $f_{use} = 1$ (see Section 3.3). In the background (green histogram) we show the distribution of photometric redshifts from the UltraVISTA catalog that were used to select the survey targets. The spectroscopic sample is relatively consistent with being drawn from the Ultra VISTA sample, but the spectroscopic redshifts more accurately reveal narrow spikes in the redhift distribution. Right: the S/N distribution, with a median $S/N = 19$ Å^{-1}.

Пример спектра

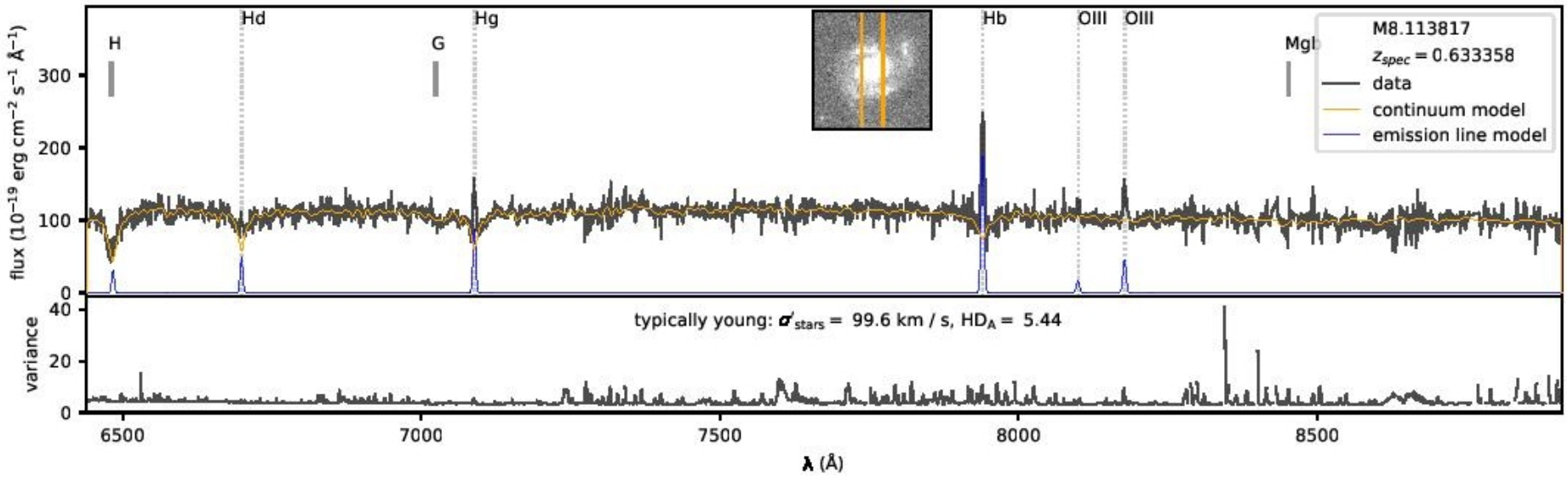

Пример спектра

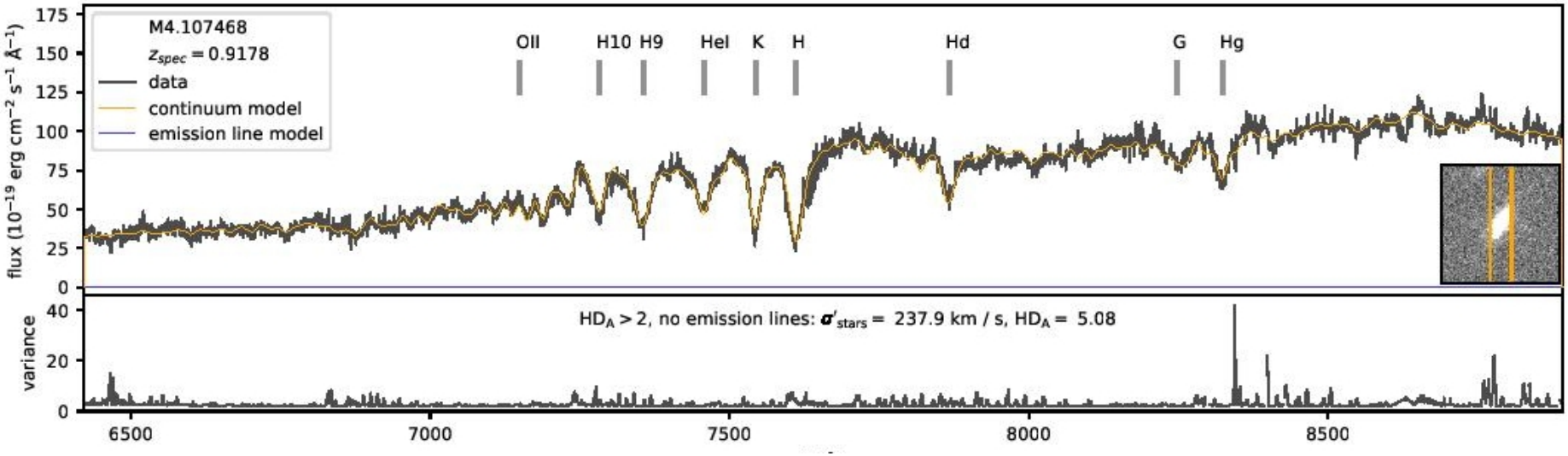

Пример спектра

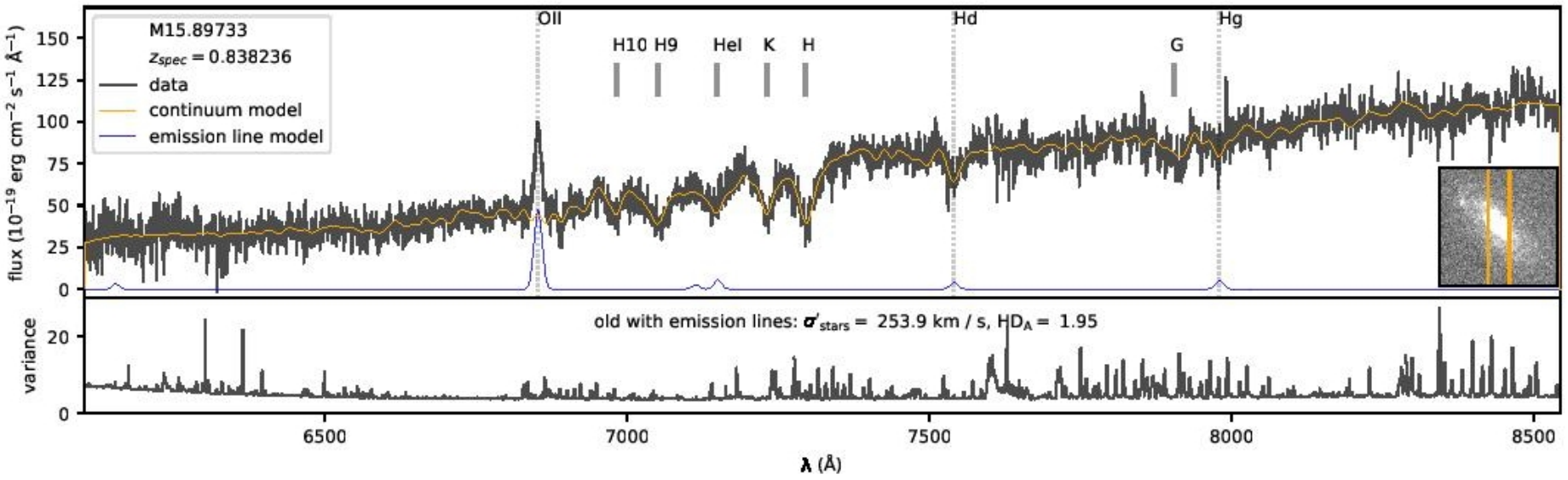

И сразу пошли неожиданные результаты: много галактик «омоложенных»

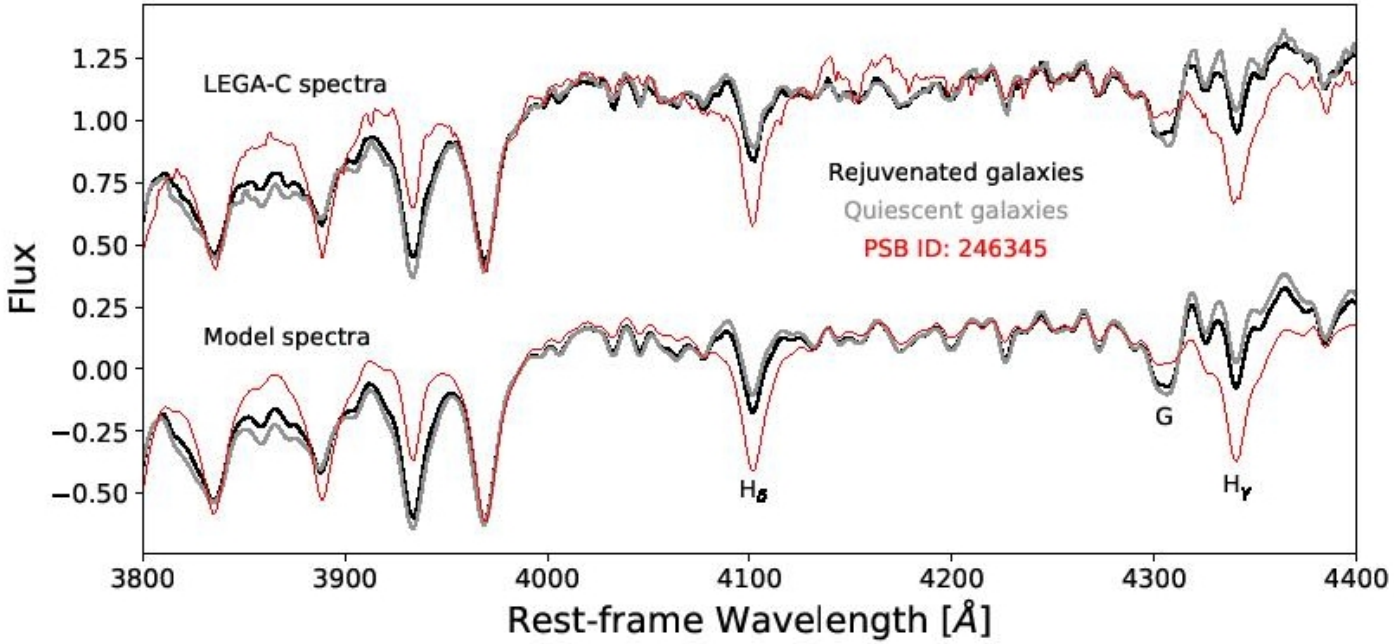

Figure 2. Average spectrum (LEGA-C as well as best-fit model) of rejuvenated galaxies (black) compared to the average spectrum of stellar mass and H_δ matched quiescent galaxies that do not show evidence of rejuvenation (gray). The PSB spectrum is shown for comparison. The spectra have been normalised and shifted for comparison purposes.

Примеры восстановленных историй звездообразования

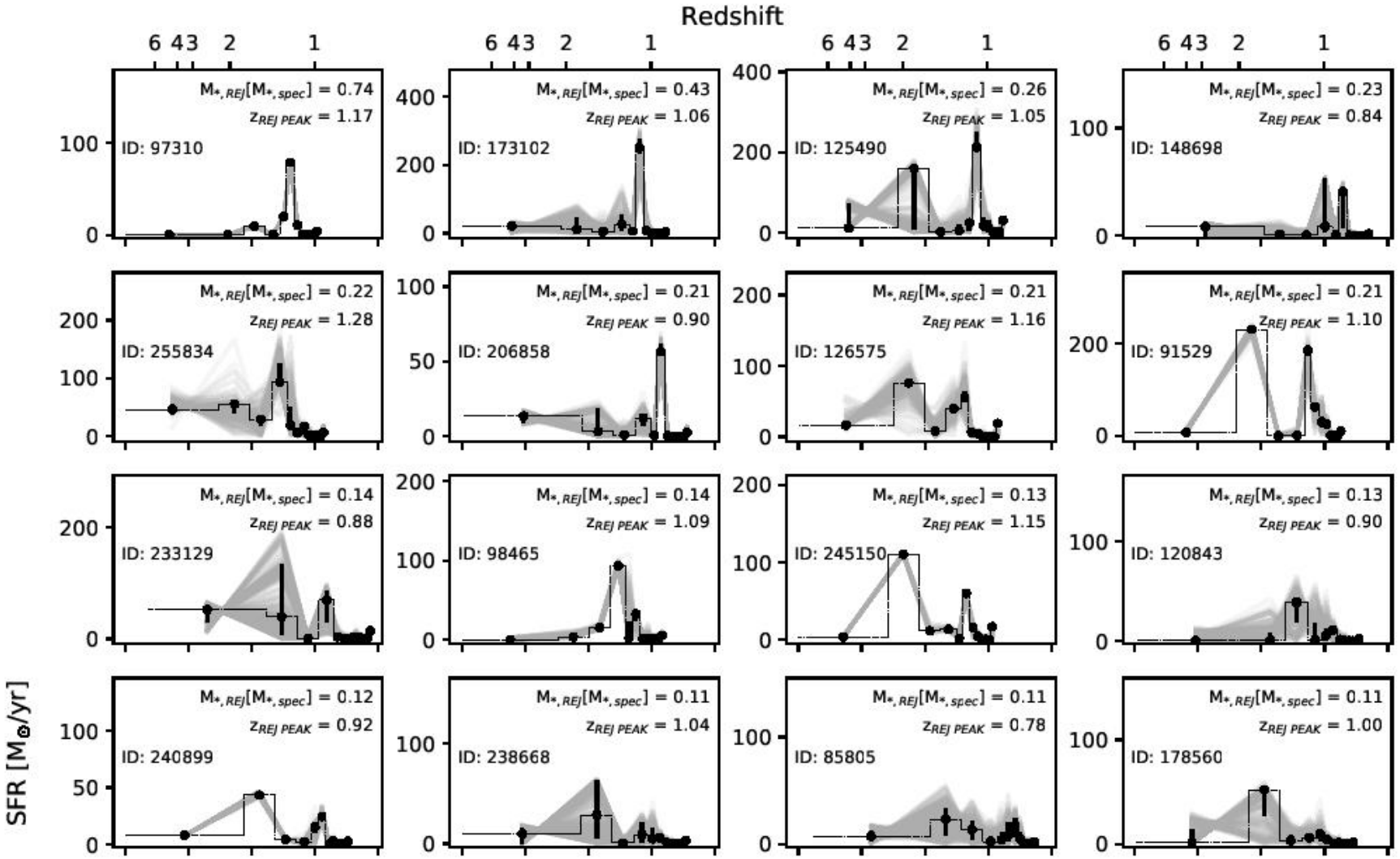

Примеры восстановленных историй звездообразования

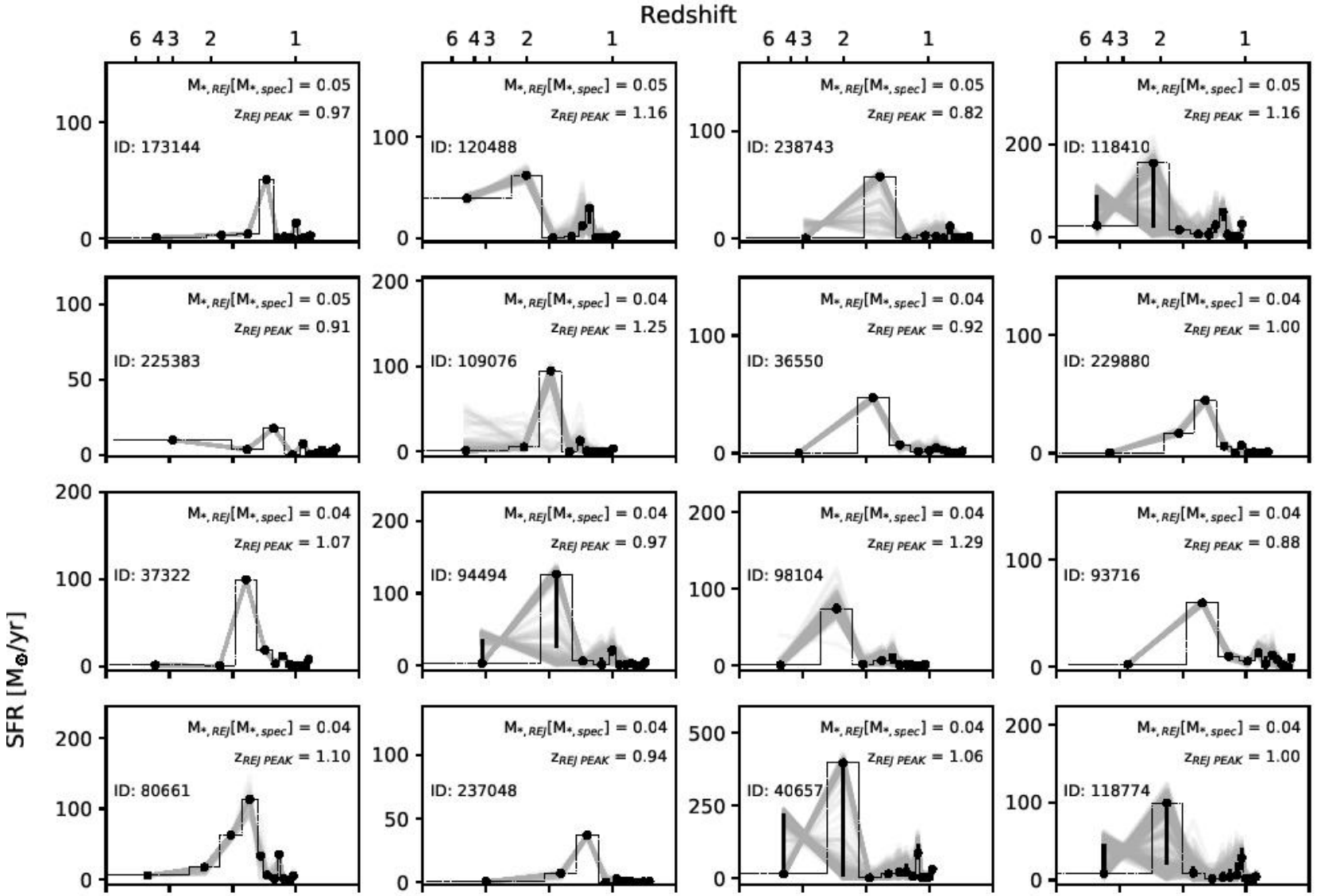

Ну, и в среднем – несколько процентов массы во вторичной вспышке образовалось

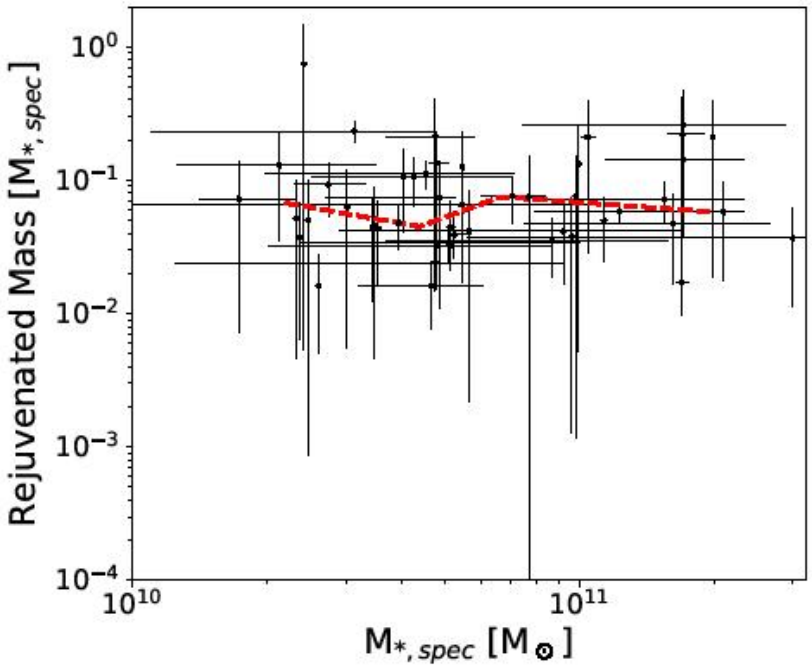

Figure 6. Stellar mass of rejuvenated galaxies versus the fraction of stellar mass from the rejuvenation event. The upper and lower uncertainties are based on the 16^{th} and 84^{th} percentiles of the walkers (see Section 2.1). The median trend is indicated in red.

И еще один неожиданный результат – доказательство множественных путей quenching'а

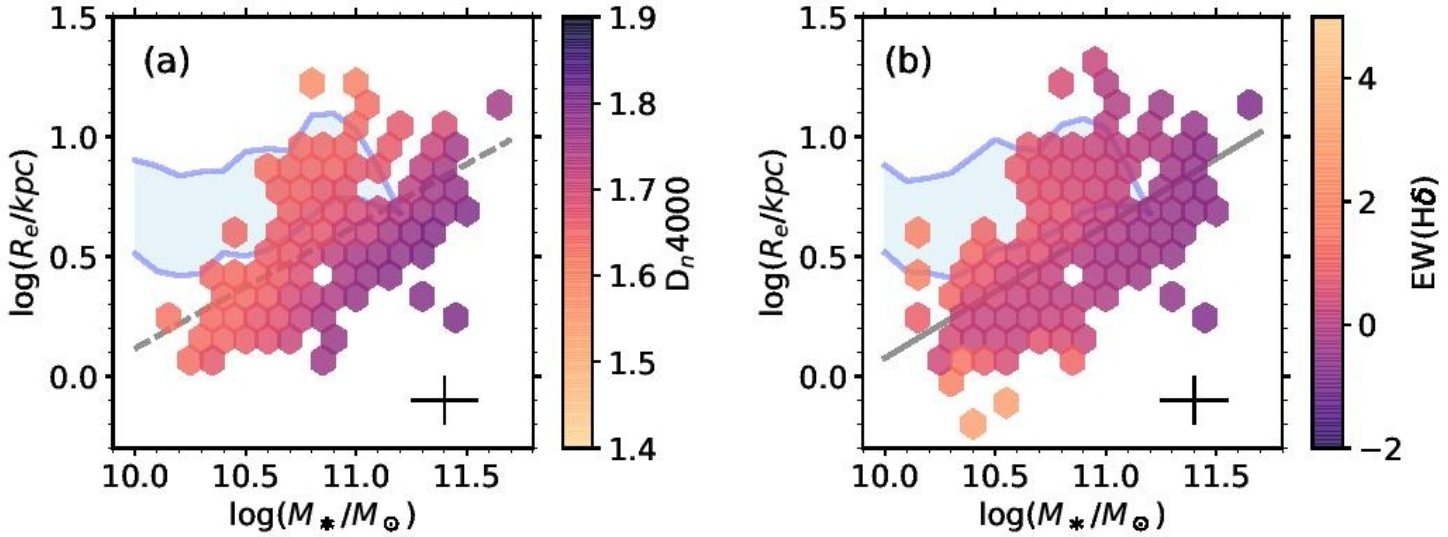

Figure 6. The D_n4000 and EW(Hδ) averaging over nearby data points on the mass-size plan using the LOESS method (see text). The smoothed maps reveal the underlying size dependence. Larger galaxies have on average smaller D_n4000 and larger EW(Hδ). However, the most compact galaxies also have large EW(Hδ), which is opposite to the general trend. The light-blue shaded areas are the 16th and 84th percentiles of the sizes of star-forming galaxies at fixed masses. The dashed and solid lines are the best-fit mass-size relations of quiescent galaxies. Dashed and solid lines are the best-fit mass-size relations of quiescent galaxies. Complementary results using other definition of quiescence are shown in Fig. 16 and Fig. 17 in the Appendix.

Еще один последний вздох на VLT VIMOS'a – VANDELS (Talia, Cullen)

- Две выборки – 681 галактика со звездообразованием в интервале $2.5<z<5.0$, полный диапазон масс, и пассивные галактики в интервале $1<z<2.5$.
- Всего 1132 спектра, из них 217 – с экспозицией >80 часов.
- Диапазон 4800-9800 АА, т.е. restframe UV → профили PCyg от оптически толстых ветров, вычитание звездного населения, и определение химии газа по линиям поглощения!

То есть для звездного населения фиттировалось все, что без линий!

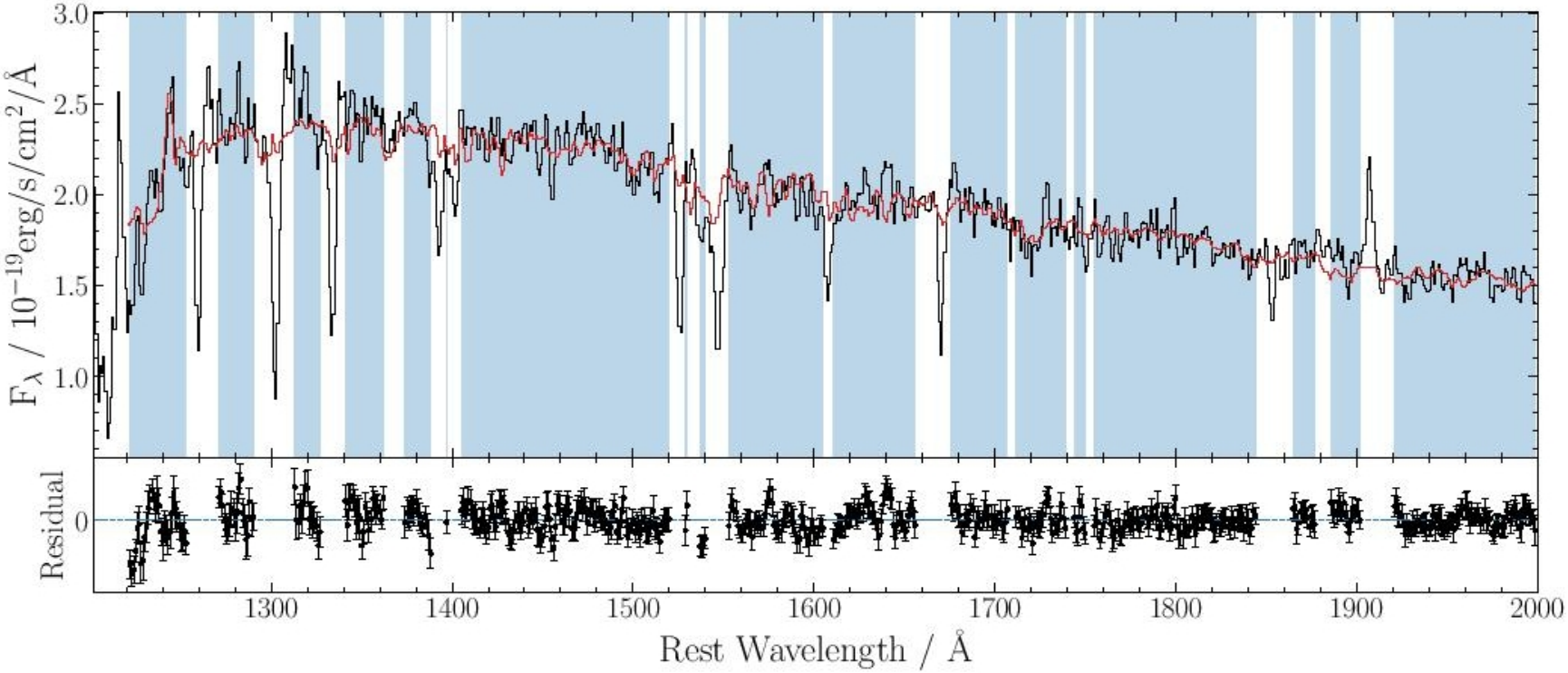

Figure 4. An example of a full spectral fit to the VANDELS-m5 spectrum (see Table 1 for details). The upper panel shows the observed composite spectrum in black with the wavelength regions used in the fitting shaded in blue. The best-fitting Starburst99 WM-Basic spectrum is over-plotted in red. The lower panel shows the fit residuals; the reduced chi-squared value for this particular fit is $\chi^2_r = 1.03$.

Примеры фиттинга

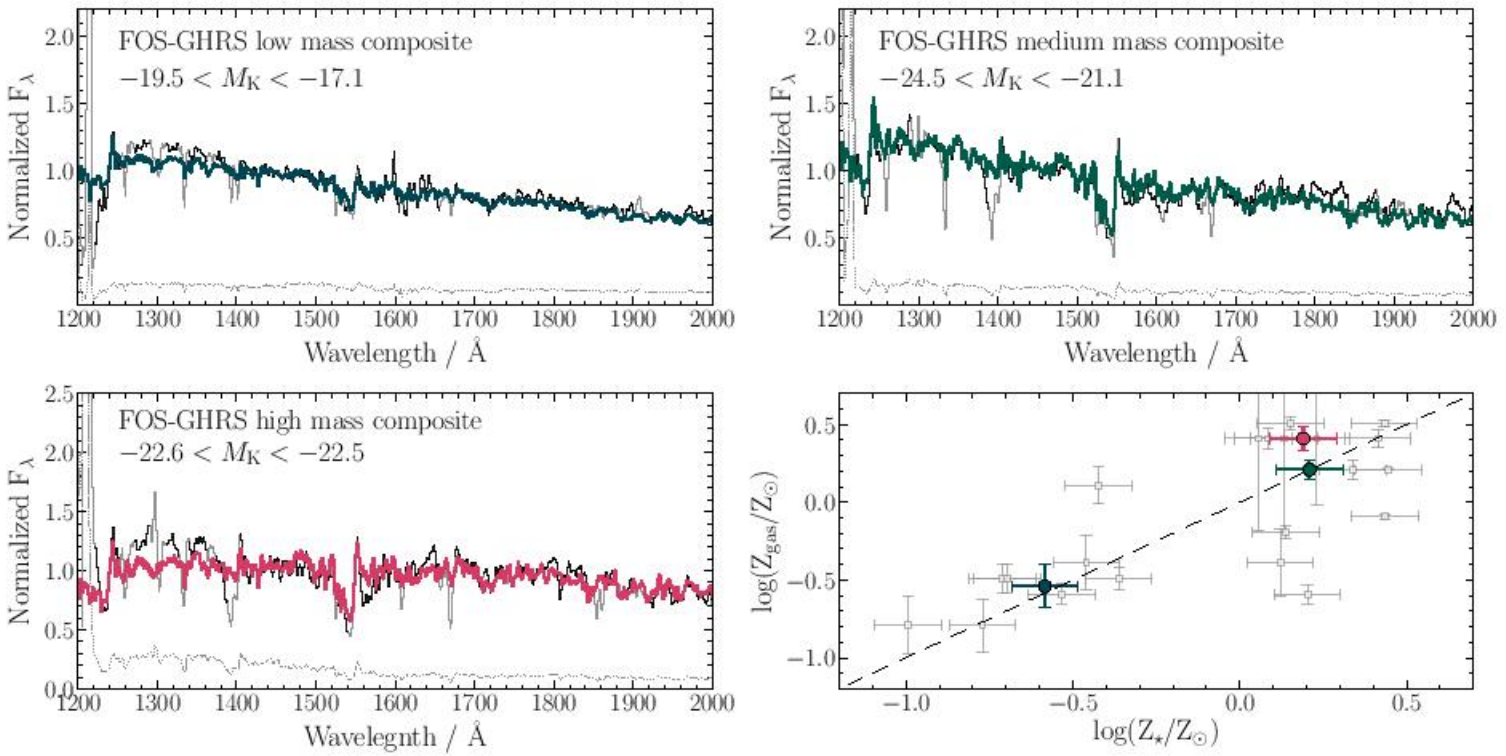

Figure 7. Composite FOS-GHRS spectra in bins of absolute K-band magnitude (M_K) with the best-fitting Starburst99 stellar population synthesis models over-plotted in colour (top two panels and lower left-hand panel). The lower right-hand panel shows the relationship between our derived stellar metallicities and published gas-phase metallicities for the FOS-GHRS galaxies, both for the individual galaxies (grey points) and the composites (coloured points), illustrating the expected correlation between these quantities (the Spearman rank correlation coefficient is 0.70).

Химическая эволюция в 4 раза?

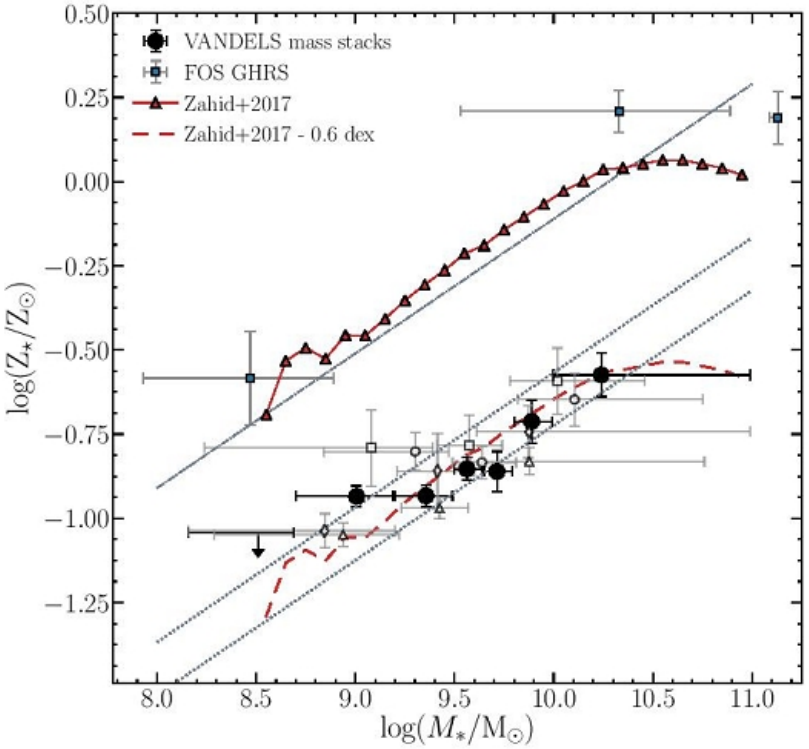

Figure 11. Redshift evolution of the stellar mass versus stellar metallicity relationship. The red triangular data points show the $z = 0$ relation derived from fitting stacked optical continuum spectra of $\sim 200,000$ star-forming galaxies in the Sloan Digital Sky Survey (Zahid et al. 2017). The blue square data points show the FUV-based stellar metallicities for the composite FOS-GHRS spectra of local star-forming regions and starburst galaxies discussed in the text. The VANDELS data at $2.5 < z < 5.0$ are shown as the black/grey data points as in Fig. 9. The dashed red line shows the $z = 0$ relation of Zahid et al. (2017) shifted by -0.6 dex in $\log(Z_*/Z_\odot)$. Simply shifting the local relation down by a factor $\simeq 4$ produces remarkably good agreement with the high redshift data. The dotted grey lines show the FIRE prediction at $z = 2.3$ (upper) and $z = 5.0$ (lower) and the grey dot-dashed line is the FIRE prediction at $z = 0$. The FIRE metallicities have been arbitrarily scaled upwards by a factor of 2 (0.3 dex).

А из этой картинки сделан вывод о повышенном отношении альфа-элементов к железу на z=3.5

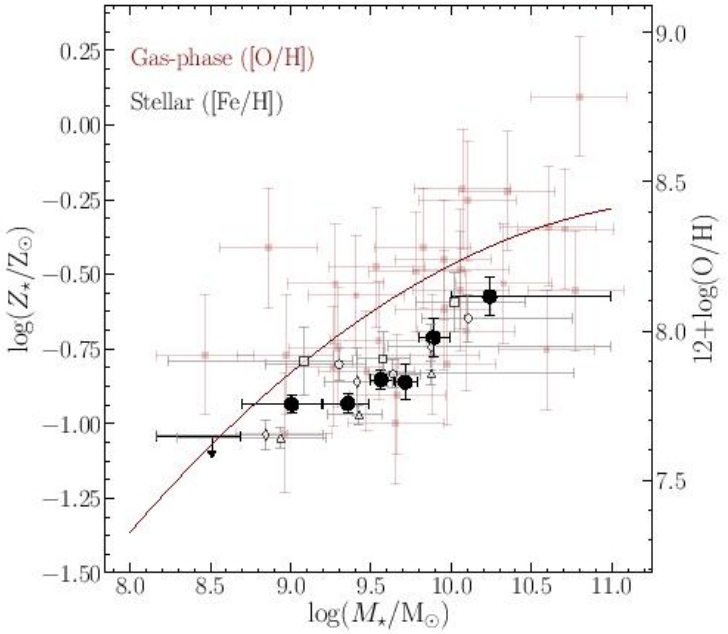

Figure 13. A comparison of the stellar and gas-phase mass-metallicity relationships at $z \sim 3.5$. The gas-phase data, tracing [O/H], are taken from the AMAZE/LSD survey of star-forming galaxies at $3 < z < 5$ with $\langle z \rangle = 3.4$ presented in Troncoso et al. (2014). The left-hand y-axis labels give metallicity in units of $\log(Z_*/Z_\odot)$ while the right-hand labels give the equivalent 12+log(O/H) units commonly used for reporting gas-phase oxygen abundances. The red square data points with error bars show the individual galaxy data and the solid red curve is their best-fitting relationship. The black/grey data points are the stellar metallicities of our VANDELS sample plotted as in Fig. 9. The comparison provides some evidence for alpha enhancement in star-forming galaxies at $z \sim 3.5$ of the order $(O/Fe) \gtrsim 1.8 \times (O/Fe)_\odot$

WEAVE WFCS (Kuchner)

- На WHT заработал широкопольный мультиобъектный спектрограф WEAVE.
- Обзор 16 скоплений до 5 вириальных радиусов – искали аккрецирующие галактики и их распределение по азимуту.
- Сняли до 6000 спектров на каждое скопление, глубина обзора до log M_*>9
- Искали филаменты; но только 50% всех галактик в окрестностях скоплений можно к ним приписать – как и в поле.

UVIT+Astrosat (K. Saha)

- Chandra Deep Field (включающее и UDHF).
- 45000 секундных изображений для двух площадок → экспозиции 30кс и 33кс
- Выглядит красиво, потому что пространственное разрешение 1” и предельные величины 27.3 FUV и 27.4 NUV.
- Есть еще десяток узких фильтров, 100-300 A.

Пленарные: Bacon

- AO на MUSE.
- 2017: на VLT/U4 поменяли вторичное зеркало на активное – 1150 точек приложения силы – убирает приземную турбулентность → 0.7’’
- 2018: Приставка к MUSE, GLAO (tip-tilt), → 0.65’’
- 2021: LTAO (tip-tilt по лазерной звезде) → 0.5’’

Пленарные: Poggianti

- GASP(MUSE): 114 jelly-fish галактик в скоплениях $0.04<z<0.07$
- Усиление в них SF на 0.2 dex; а в хвостах – только 2%-5% от звездообразования галактики
- BPT-диаграммы: в среднем 50% хвостов – DIG; а у NGC 4569 весь газ в хвосте – DIG
- Повышенная встречаемость активных ядер

Динамика галактик: тоже обзоры

- HIX (K. Lutz): отбор галактик с повышенным содержанием нейтрального водорода (для их массы повышена SF и понижена металличность) и картирование в 21 см
- При обычной поверхностной плотности – более протяженные диски HI. Повышенный момент гало? Стабилизирует HI.

Выборка HIX

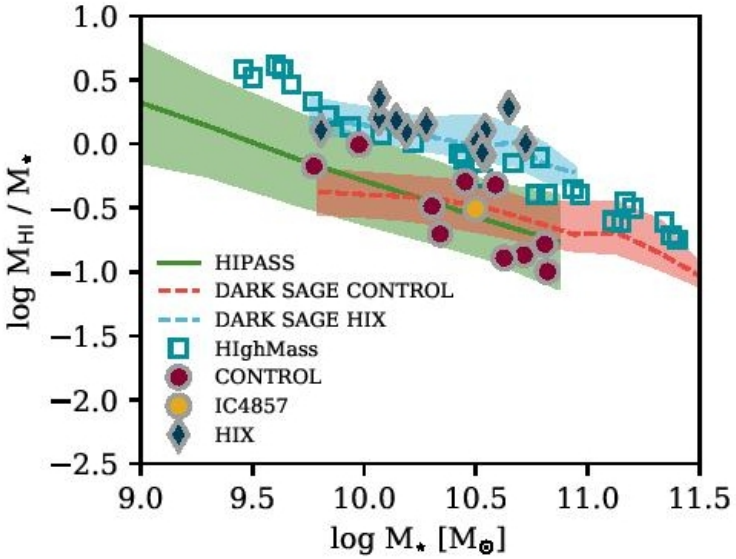

Figure 1. The H I–to–stellar mass ratio as a function of the stellar mass. The green shaded area shows the 1 σ range of the parent sample (with 2MASS cross match), red circles give the control sample and blue diamonds represent the HIX sample. The yellow circle is IC 4857, which was initially selected as a HIX galaxy, but then reclassified to a control galaxy. The empty blue squares present the HIghMass sample. Orange and light blue dashed lines indicate the running average of simulated HIX (light blue) and control galaxies (orange) from the DARK SAGE semi-analytic model (for more details see Sec. 4). The orange and light blue shading covers the 16 to 84 percentile range. As per sample selection, HIX galaxies have high H I mass fractions for their stellar mass.

Повышенная масса HI – из-за большого диаметра диска

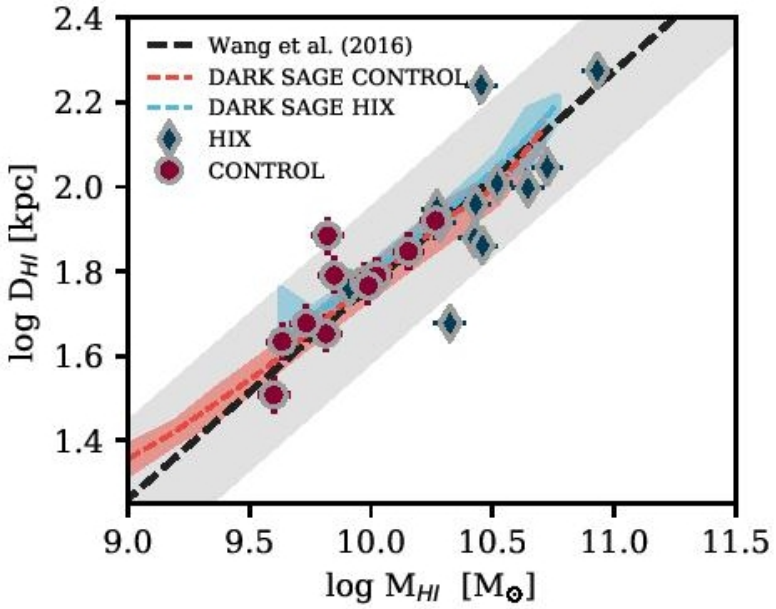

Figure 3. The relation between H I disc size and mass. Blue diamonds present the HIX sample and red circles the control sample. The grey dashed line is the relation found by Broeils & Rhee (1997), confirmed by Wang et al. (2016), where the grey shaded area covers their 3σ scatter of 0.18 dex. As in Fig. 1 light blue and orange dashed lines present DARK SAGE simulated galaxies and the shaded areas their respective 16 to 84 percentile ranges. H I masses and sizes of the HIX galaxies are consistent with the literature relation.

А вот другая выборка – с пониженным количеством газа

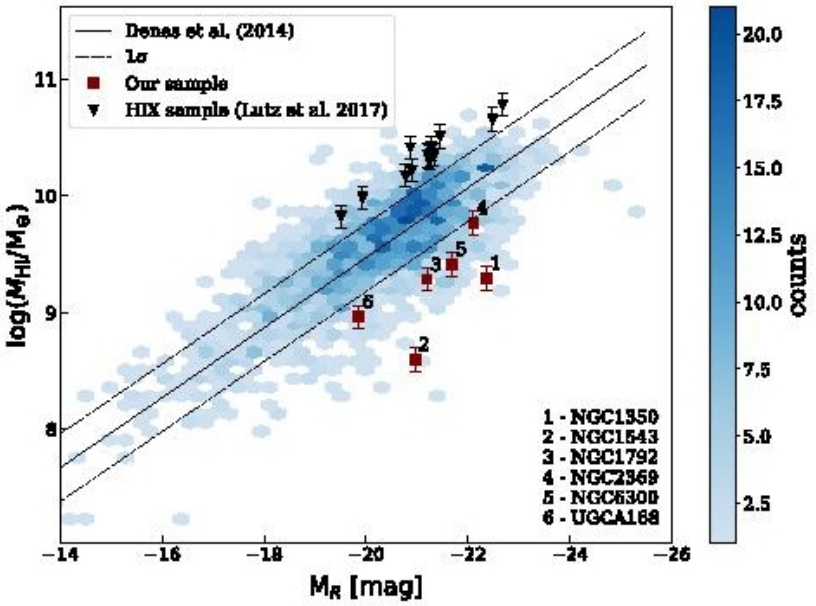

Figure 1. The $M_{\rm H\,I} - {\rm M}_R$ scaling relation from Dénes et al. (2014) for over 1700 HIPASS galaxies from the HOPCAT catalogue. The colourbar shows the number density of galaxies within each hexagon in the plot. The maroon squares represent the current sample of H I-deficient galaxies. In contrast, also shown in black (inverted triangles) are the H IX sample of H I-excess galaxies from Lutz et al. (2017).

Все радостно сводят к устойчивости по Крумхольцу

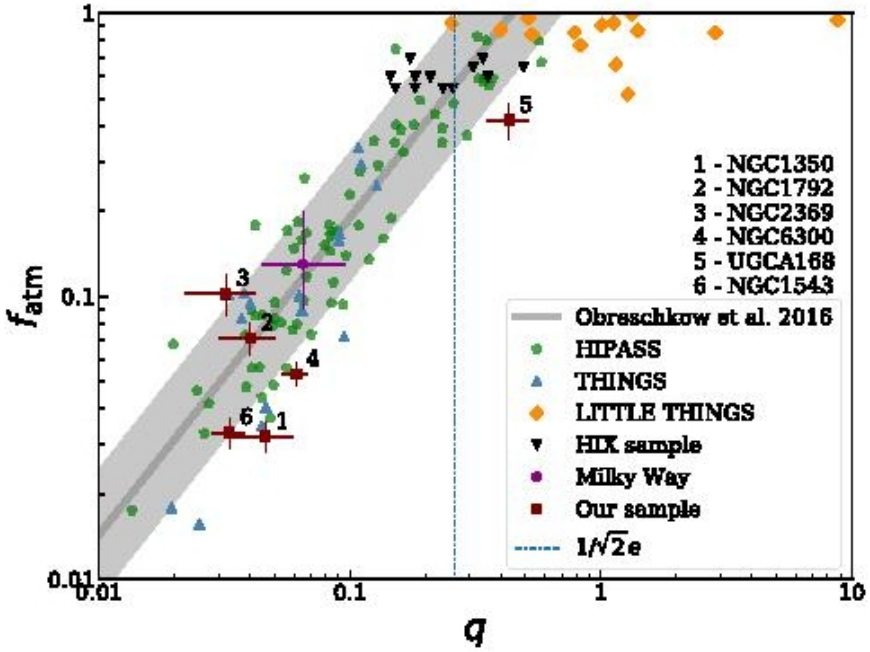

Figure 3. The $f_{atm} - q$ relation. The galaxies in our sample are represented by the maroon squares. The dark gray line is the analytical model for f_{atm} from O16. The shaded gray region shows the 40% scatter about the model. Also shown are galaxies from THINGS, LITTLE THINGS, HIPASS and the HIX surveys. The vertical dotted line represents $q = 1/\sqrt{2}e$, the threshold beyond which axially symmetric exponential disks of constant velocity can remain entirely atomic.